# Ray Casting Approach for Boundary Extraction and Fourier Shape Descriptor Characterization

Joel Rosiene[a], Xin Liu[b], and Celina Imielinska[b]

[a]Department of Mathematics and Computer Science,Eastern Connecticut State University, Willimantic CT

[b]Department of Biomedical Informatics,Columbia University, NY, NY

## ABSTRACT

There are many significant applications of Fourier Shape Descriptor characterization of boundaries of regions in images. Whenever it is desirable to compare two shapes, independent of rotation, starting point, or compensate for magnification, Fourier Shape Descriptors (FSDs) have merits.[1] FSDs have been proposed for the automatic assessment of packaging; to check alignment of objects for automation; and characterize visual objects in video coding, and compare biomedical regions in medical images. This paper presents a technique to parameterize the boundary of the region of interest ($ROI$) that utilizes the casting of rays from the center of mass of the region of interest outward to points in the image that lie on the edge of the $ROI$. This is essentially another technique to obtain the R-S parametrization. At each step the process utilizes the sections of the boundary have radii that are a simple function of theta. The procedure then merges these simple boundary sections to create a periodic complex valued function of the boundary parameterized by a parameter $s$ that is not required to be a function of theta. Once the complex periodic sequence is obtained, the Fourier Transform is taken resulting in the corresponding Fourier Shape Descriptors. Since the technique seeks the intersection of a known ray with the boundary (it is not boundary following), the worst-case behavior of the technique is easily calculated making it suitable for real-time applications. The technique is robust to incomplete boundaries of objects, and can be readily extended to three-dimensional datasets (spherical harmonics). The a simpler version of the technique is currently being used in the automatic selection of the axis of symmetry in Magnetic Resonance Images of the brain, and we will demonstrate the application of the technique on these types of datasets, although the technique has general application.

## 1. INTRODUCTION

The value of Fourier Shape Descriptors is well known.[1] One step in the calculation of the Fourier Shape Descriptors is the calculation of the complex valued function $f(s) = x(s) + iy(s)$ where $s$ is the arc length and $x(s), y(s)$ is the location of the curve at the point $s$ treated as a complex number. For a closed curve this function is periodic. The Fourier Shape Descriptors are simply the complex valued Discrete Fourier Transform coefficients.

In the medical application being explored, the boundary of anatomic structures in brain imagery are being segmented by a ray casting technique and it is natural to extract information of the boundary from the rays.[2] For example, the convex hull is trivially extracted since the rays are cast from the centroid of the object form the "star shaped object" used in the formation of the convex hull.

In this generation of the technique, by recording all of the intersections of the boundary with the ray, we generate the boundary as a function of $s$. This is essentially a different approach to obtain the R-S representation of the boundary[3] which might be of some interest.

## 2. TECHNIQUE

The technique follows rays ($r(\theta)$) emanating from the centroid $(cx, cy)$ of the contained in the region of interest ($ROI$). The intersections of the ray with the boundary of the region are recorded. * Obviously, when the



Computational Imaging III, edited by Charles A. Bouman, Eric L. Miller,
Proceedings of SPIE-IS&T Electronic Imaging, SPIE Vol. 5674

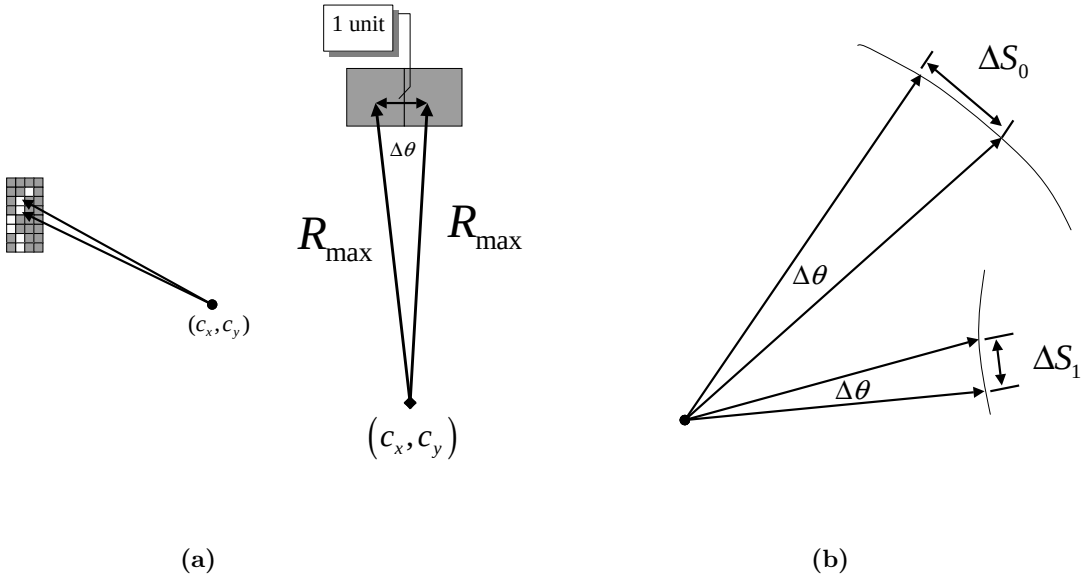


**Figure 1.** Ray extending from the centroid of the object (a), change in arc length from one pair of adjacent intersections to the next

centroid is interior to the ROI all of the points on the boundary are path connected to centroid,[4] and a ray extending from the centroid (a straight path) will intersect at least one point on the boundary.

The rays are parameterized by the discrete approximation to $\theta = k\Delta\theta,\ k \in Z$ is used. The value of $\Delta\theta$ is chosen as in the figure to insure that the step doesn't exceed $\sqrt{2}$ at a given maximum radius (As in Figure 1, worst case behavior is when the boundary is diagonally connected). For example, by selecting the points furthest away from the centroid this constructs the star shaped object, with each of the rays indexed by $r(k\Delta\theta)$.[1,5]

PROPOSITION 2.1. *All boundaries of objects can be represented as a sequence of functions $r_j(k\Delta\theta)$ that parameterize the radii by theta, possibly discontinuous, relative to an interior point,where $j$ indicates the $j^{th}$ boundary stopping points furthest from the centroid. When there is no closer boundary point, the furthest stopping point is selected.*

The stopping point of the ray can be enumerated as follows:

**Exterior to Interior** Tracing the ray back toward the centroid, the there is a transition from exterior to the interior of the object. This is the first transition.

**Interior to Exterior** Tracing the ray back toward the centroid, the there is a transition from the interior to the exterior of the object. This can not be the first transition.

**Coincident with the Boundary** The ray passes through boundary elements which are inline with the edge (See figure 5)

The $j$ index in $r_j(k\Delta\theta)$ indexes the stopping point of the ray, starting at the boundary point furthest from the centroid, and working inward.

Each of these curves (that partition the path connected boundary points) will share points that will allow us to traverse the true boundary of the object. We refer to this as the *mesh* of functions which contain the true

*In this paper, we only consider the case when the centroid is contained inside the body of the object, but the technique can be extended to include the case where the centroid lies outside of the region of interest.

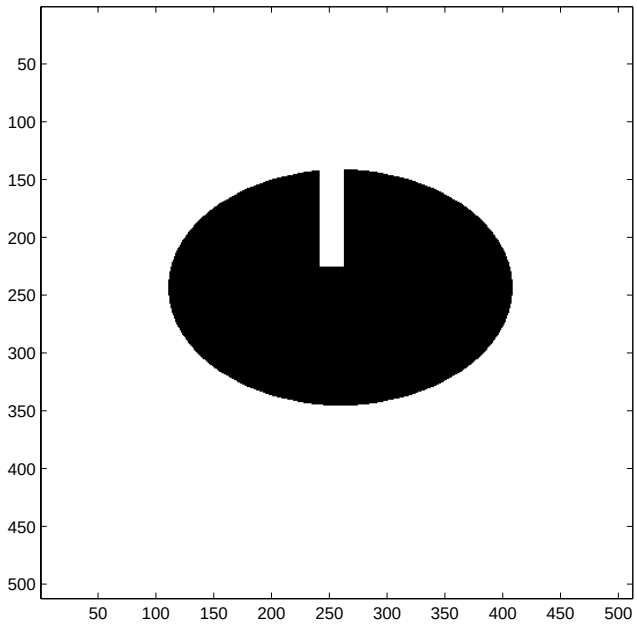


**Figure 2.** Representative Boundary. A ray extending from the centroid will pass through the boundary at least once. In the region of the notch, the ray will pass through multiple times. Three of the intersections are shown below.

boundary. Starting at a point on the first function of theta, (e.g., on the set of points furthest away from the centroid) the boundary will be connected to the other sections of the boundary in the following manner.

PROPOSITION 2.2. *The true boundary of the object can be extracted from the "mesh" by selecting the next point, closest and adjacent to the current point in delta_theta ( positive or negative ) of less than* $\sqrt{2}$.

The maximum change of $\sqrt{2}$ is obtained from allowing the boundary to be 8-way connected,[1,3] which it turn, is related to the angular step-size through the maximum distance to the centroid of the object.

Since the $\Delta\theta$ was chosen to insure the rays pass through adjacent pixels, and it is assumed the boundary is complete, at a change of radius exceeding $\sqrt{2}$ the next point of minimum radius will lie on the curve formed from the second intersection of the ray and the boundary, or a collocated ray.

The algorithm to form the curve is from multiple boundary curves is given in Figure 4. Starting at any point on the boundary, the curve is traversed in a given direction, until there is a discontinuity. Since the assumption is we have a complete boundary, and the sampling in angle was selected to insure one sample of adjacent pixels at maximum radius, the distance between adjacent points on the boundary shouldn't exceed $sqrt2$. If this distance is exceeded then the next boundary point will been recorded on an adjacent curve. Both the intersections closer to the centroid and further from the centroid are checked in turn, and collocated points handled.

Notice, that if the boundary is incomplete, leading to a ray (or rays) which is not 8-way connected we can selectively "skip" the point and search for the next point which satisfies some prior assumption about the boundary (curvature, size, etc..). In this way, the technique differs from boundary following, although the authors concede that it is common practice to extend boundary following techniques to allow for gaps, or use other approaches to complete the boundary prior to representation.

All points intersecting the ray will be recorded on one of many curves, and there may be many curves resulting from collocated points. To reduce the number of curves required, we can restrict the class of objects, by relaxing the requirement for 8-way connectedness, increasing the maximum change into radius permitted beyond $\sqrt{2}$ to allow sub-sampling of the edges collocated with ray.

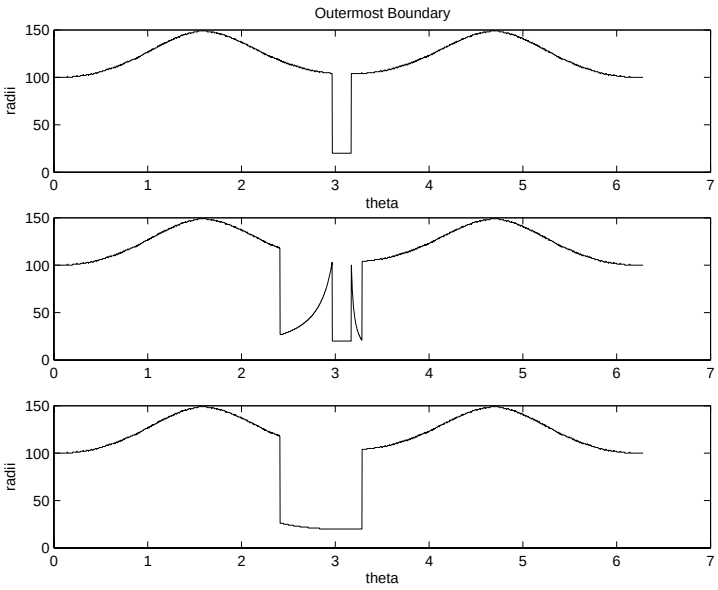


**Figure 3.** Three curves representing the mesh of the boundary ray intersection stopping at decreasing radii. The upper most curve is constructed from the outermost intersection of the ray and the boundary, the lowermost curve is constructed from the intersections closest to the centroid

In the example being considered, figure 6 is the boundary due to the merging of the curves according to the above algorithm. The restriction to the object was made to limit the number of boundary curves. However, by allowing for larger changes in the radius the algorithm will not be correct for all boundaries. By allowing changes in radius greater than $\sqrt{2}$ it is possible to have continued on the same curve if the radius doesn't change more than a given amount (in this case 10). In some boundaries, this increase in allowable change in radius may connect sections of a curve which should be unconnected. The recovered boundary, both the radii and the associated angle are plotted verses arc length in figure 6.

This approach leads to a finite subdivision of the interval of the domain of the curve, which is piecewise approximated by straight line segments (in what follows we use the standard treatment[6]). For our case, after the algorithm completes we have $P_0 = \mathbf{boundary}(1), P_1 = \mathbf{boundary}(s)$ on the interval $[1, s], \Sigma : 1 < 2 < 3 < \cdots < s$ with line segments $\mathbf{boundary}(k)\mathbf{boundary}(k+1)$. We can estimate the length of the arc as

$$L(\Sigma) = \sum_{k=1}^{s-1} | \mathbf{boundary}(k+1) - \mathbf{boundary}(k) |$$

.

As in the standard definition of arc length "as a limit of lengths of polygonal curves inscribed into an arc".[6] We can use a standard interpolation or curve fitting technique to extend the value of the boundary at the points of the subdivision to the entire interval to obtain a model of the boundary as a function of arc length.

The distance (see Figure1) between the ray intersections are irregularly spaced in discrete samples of arc length $s$ and the care should be taken to interpolate to a regular spacing, or iterate to the correct Fourier coefficients.[7] With care, this step provides a degree of scale independence subject to the underlying resolution of the image. The ability to represent the boundary independent of scale is related to the underlying resolution of the image, since we are sampling the boundary on a regular grid.

Each of the $r(s)$ have an associated angle $k\delta\theta$ from which the position of the point is obtained (see Figure7a). Treating these points as complex values in the normal manner leads to the Fourier shape descriptors. Figure7b

1. set curve to 1, set point to 1,set direction to clockwise, set s to 1
2. do
3. while($\|next\_point(curve, point, direction) - current\_point(curve, point)\| <= \sqrt{2}$)
4. boundary(s) $\leftarrow current\_point(curve, point)$
5. point $\leftarrow$ next_point(point,direction)
6. $s \leftarrow s + 1$
7. end while
8. set direction to reverse(direction)
9. if ($curve < max\_curve$) then
10. if ($\|current\_point(curve, point) - current\_point(curve + 1, point)\| <= \sqrt{2}$)
11. while($\|next\_point(curve, point, direction) - current\_point(curve, point)\| >= \sqrt{2}$)
12. boundary(s) $\leftarrow current\_point(curve, point)$
13. curve $\leftarrow$ curve + 1;
14. $s \leftarrow s + 1$
15. end while
16. end if
17. end if
18. if ($curve > 1$) then
19. if ($\|current\_point(curve, point) - current\_point(curve - 1, point)\| <= \sqrt{2}$)
20. while($\|next\_point(curve, point, direction) - current\_point(curve, point)\| >= \sqrt{2}$)
21. boundary(s) $\leftarrow current\_point(curve, point)$
22. curve $\leftarrow$ curve - 1;
23. $s \leftarrow s + 1$
24. end while
25. end if
26. end if
27. until (curve = 1) and (point = 1):
28. End;

**Figure 4.** Algorithm to Convert from a Sequence of Simple Functions to the Boundary, the point structure records both the radius and the angle or the x and y position which ever is more convenient for the application. The $\|\cdot\|$ is the $l^2$ norm.

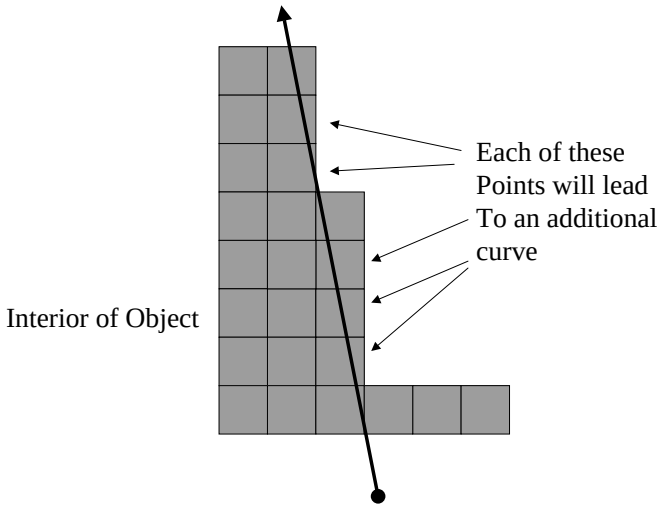


**Figure 5.** A ray which intersects multiple pixels on the edge.

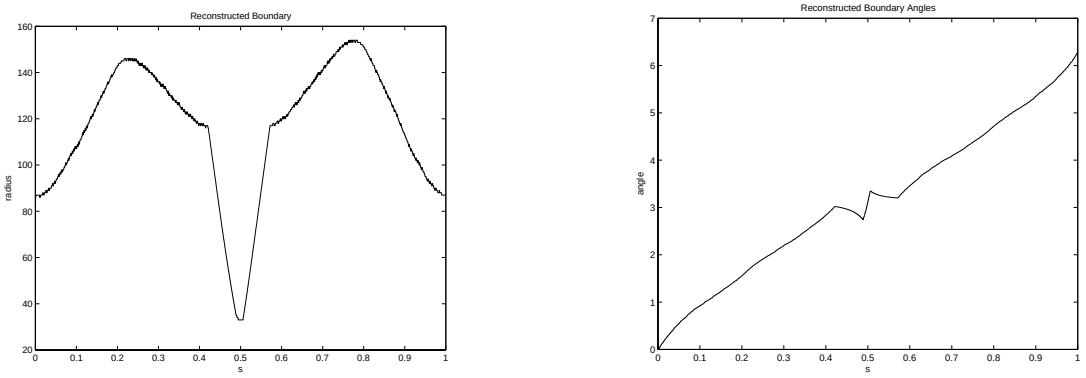


**(a)** **(b)**

**Figure 6.** The radii of the recovered boundary (a), and angles(b)

presents the magnitude of the Fourier shape descriptors. The first term in the magnitude plot relates to the average of the complex numbers representing the boundary. Due to the cut in the otherwise symmetric object, this number is non-zero.

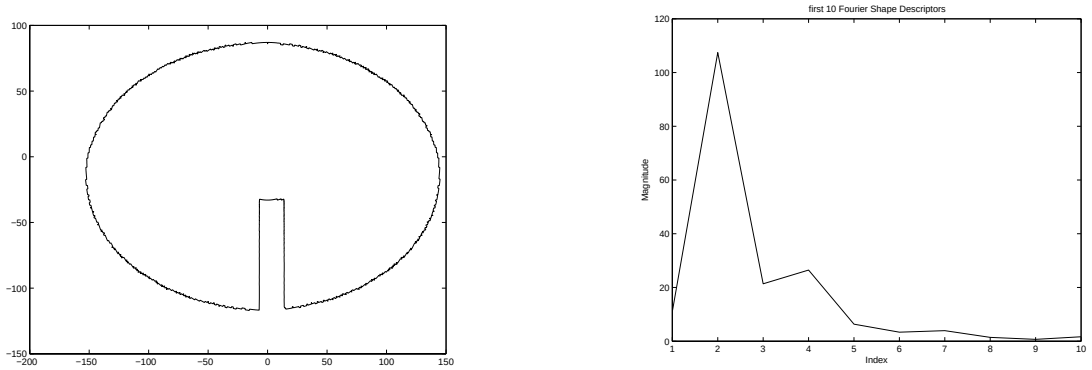


**(a)** **(b)**

**Figure 7.** The boundary represented as complex numbers (a) The first 10 Fourier Shape Descriptors (b)

## 3. APPLICATIONS

For two dimensional data Fourier shape descriptors, and for three dimensions Spherical Harmonics are used. In medical images there are numerous applications of fourier shape descriptors and spherical harmonics, for example the characterization of the brain ventricles[8].[9]

One application of the technique is to employ the automated symmetry computation in assessing proper alignment of patient head in the scanner (e.g. MR scanner). The boundary of the region of interest is detected (.e.g. by simple thresholding) and the technique is used to extract the boundary. We have been involved in testing the following applications:

1. 2D CT Brain Perfusion. Quantification of perfusion-weighted computed tomography in the setting of subarachnoid hemorrhage.[10] We quantify (a)symmetry of perfusion-weighted parameters (e.g. cerebral blood flow) using automated computation of axis of symmetry, automated delineation of vascular territories, that is a direct application of the technique described in this paper.

2. 3D MR Brain Perfusion. Quantification of the degree of relative difference between corresponding vascular regions in the ipsilateral and contralateral hemispheres by taking the relative difference in brain perfusion between these two sides, for patients who underwent carotid endarterectomy (CEA) (who had significant carotid artery stenosis).[11]

In a more sophisticated way, the actual brain region can be segmented using a fast segmentation method and the boundary shape of the brain matter is used to detect images that are not aligned to the coordinate system of the imaging system. In Figure 8, we show an example of brain MR PD and T2 data, Figure 8(a) and Figure 8(b), respectively that is segmented by a hybrid segmentation method, Figure 9(a), and its 3D corresponding model is extracted, Figure 9(b). Using such segmented data of the brain region, and selecting two/three sample segmented slices in the volume, we can apply our method to derive corresponding FSDs, compute axis of symmetry in each slice and fit a plane of symmetry for the brain. From the plane of symmetry we can assess the degree of alignment of the patient's head within the coordinate system of the scanner.

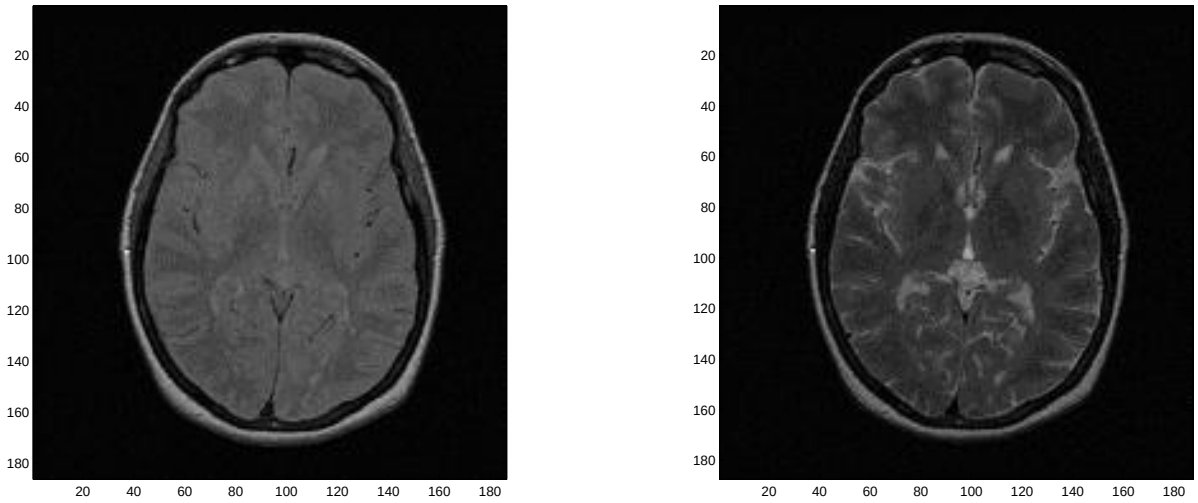


**(a)** **(b)**

**Figure 8.** Input volumetric data of brain region: (a) MR PD image (a single slice shown in a volume); (b) MR T2 slice in the volume.

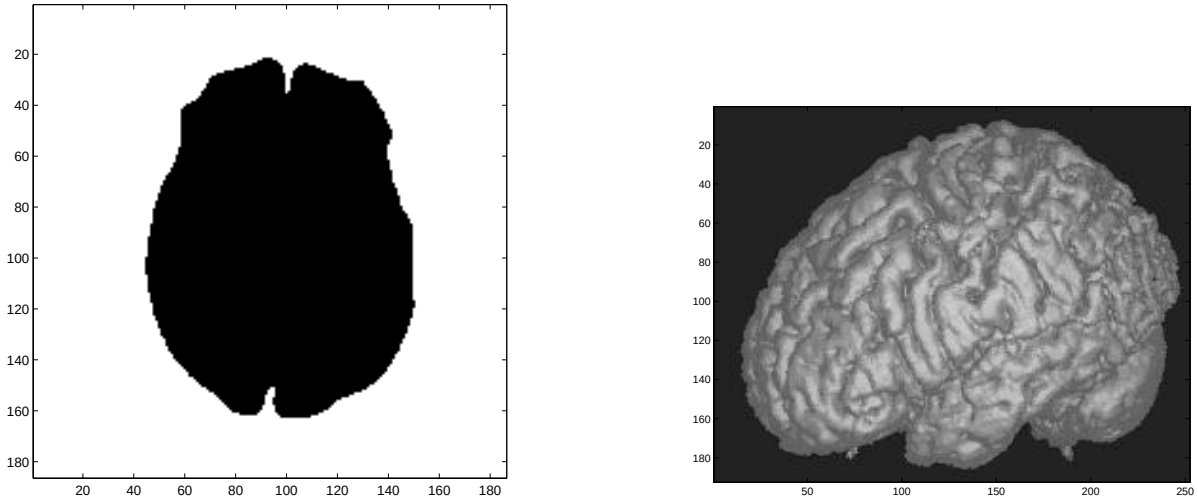


**(a)** **(b)**

**Figure 9.** Segmentaion of brain MR PD and T2 data using hybrid segmentation method that combines fuzzy connectedness, Voronoi Diagram classification and deformable models[12,13]: (a) segmented image in the volume; (b) corresponding 3D model.

## 4. COMPLEXITY

The number of rays cast is a constant $\frac{2\pi}{\Delta\theta}$ while the number of intersections with the sampled boundary is based on the number of true boundary points of the object. The merging of the curves requires on the order of the number of points on the boundary, since all points are visited only once.

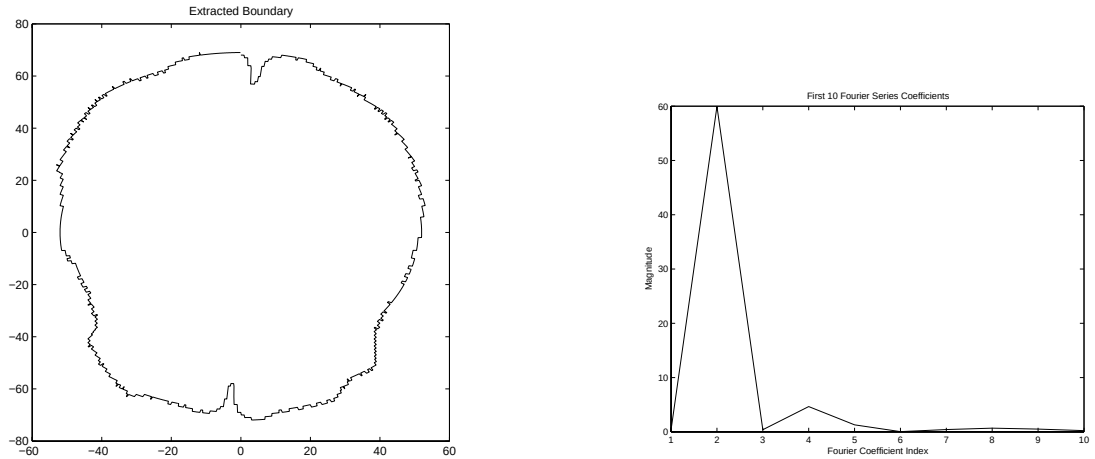


**(a)** **(b)**

**Figure 10.** The reconstructed boundary (a) Fourier Shape Descriptors of the boundary (b)

## 5. CONCLUSION

A mechanism to construct the boundary of a region of interest, when the centroid of the region of interest is internal, has been presented. The resulting boundary representation from application of the technique is not new, but provides an alternative to boundary tracing. An attempt to identify the sources of errors in the estimated Fourier Shape Descriptors has been made.

The technique can be extended to three dimensions and regions of interest homomorphic to the sphere, with the obvious generalizations to the solid angle and spherical harmonics.

## REFERENCES

1. R. Gonzalez and R. Woods, *Digital Image Processing*, Addison-Wesley, 3rd ed., 1993.
2. X. Liu, J. Rosiene, and I. Greenshields, "Anatomically based algorithmic segmentation of kidney imagery," in *Proceedings of the 4th Visible Human Conference*, (Keystone, Colorado), October 2002.
3. B. S. Morse, "Lecture 7: Shape description (contours)." "http://homepages.inf.ed.ac.uk/rbf/", January 2002. "CVonline//LOCAL_COPIES//MORSE//boundary-rep-desc.pdf".
4. S. G. Hoggar, *Mathematics for Computer Graphics*, ch. 12.2, pp. 287, 300. Cambridge University Press, 1992.
5. D. Cox, J. Little, and D. O'Shea, *Using Algebraic Geometry*, pp. 290–292. No. 185 in Graduate Texts in Mathematics, Springer, 1998.
6. H. W. Guggenheimer, *Differential Geometry*, ch. 2, pp. 15–17. Dover, 1977.
7. H. Feichtinger, K. Groechenig, and T. Strohmer, "Efficient numerical methods in non-uniform sampling theory," *Numerische Mathematik* **69**, pp. 423–440, 1995.
8. P. Golland, *Statistical Shape Analysis of Anatomical Structures*. PhD thesis, Massachusetts Institute of Technology, 2001.
9. G. Gerig, M. Styner, D. Weinberger, D. Jones, and J. Lieberman, "Shape analysis of brain ventricles using spharm," in *IEEE Workshop on Mathematical Methods in Biomedical Image Analysis (MMBIA)*, pp. 171–178, IEEE Computer Society, December 2001.
10. C. Imielinska, X. Liu, M. Sughrue, E. Hagiwara, E. Connolly, and A. D'Ambrosio, "Objective quantification of perfusion-weighted computer tomography in the setting of acute aneurysmal subarachnoid hemorrhage," pp. 34–43, Computer Assisted Radiology and Surgery, June 2004.

11. X. Liu, C. Imielinska, J. Rosiene, and et. al., "A novel quantification method for determining previously undetected mr perfusion changes in patients with cognitive deficits following carotid endarterectomy," in *Medical Imaging*, SPIE, February 2005.
12. C. Imielinska, D. Metaxas, J. Udupa, Y. Jin, and T. Chen, "Hybrid segmentation of anatomical data," **Vol. 2208 (1)**, pp. 1058–1066, MICCAI 2001 Conference, (Utrecht, The Netherlands), October 2001.
13. C. Imielinska, J. Udupa, D. Metaxas, Y. Jin, E. Angelini, T. Chen, and Y. Zhuge, *Insight into Images: Principles and Practice for Segmentation, Registration, and Image Analysis*, ch. Hybrid Segmentation Methods. A.K. Peters, March 2004.